Adsorption 11: 145–149, 2005
© 2005 Springer Science + Business Media, Inc. *Manufactured in The Netherlands.*

Comparison of $AgNO_3$/Clay and $AgNO_3$/ALSG Sorbent for Ethylene Separation

SOON-HAENG CHO*, JONG-HO PARK, SANG-SUP HAN AND JONG-NAM KIM
Separation Technology Research Center, Korea Institute of Energy Research, 71–2, Jang-dong, Yuseong-gu, Daejeon, 305–343, Korea
soonhcho@kier.re.kr

Abstract. Two π-complexation adsorbents, $AgNO_3$/clay and $AgNO_3$/ALSG, were prepared by dispersing $AgNO_3$ on clay and aluminosilica substrate, respectively. Incipient wetness method was used in preparing the adsorbents. Adsorption capacities of $AgNO_3$/ALSG and $AgNO_3$/clay for ethylene at 25 ^{o}C and 1 atm were 1.81 mmol/g and 1.26 mmol/g, respectively. Binary adsorption measurement shows that the selectivity of $AgNO_3$/ALSG for ethylene at total pressure of 900 mmHg and 25^{o}C was twice as high as that of $AgNO_3$/clay in the composition range of C_2 gas mixture of practical importance. The performance of $AgNO_3$/ALSG has been compared with that of $AgNO_3$/clay by simulating a 3-bed VSA process. The simulation revealed that the recovery with $AgNO_3$/ALSG was higher by 4% at the purity of 99.9% than that with the $AgNO_3$/clay.

Keywords: silver nitrate, adsorption, π-complexation, ethylene, pressure swing adsorption

1. Introduction

Ethylene is the most important building block in any petrochemical industry. Steam cracking of naphtha or ethane is the main route of the ethylene production. In the cracked gas, a number of components are present. Separation of ethylene from the cracked gas is the essential step of ethylene production. The separations of ethylene from ethane and propylene from propane have been achieved conventionally by low temperature and/or high-pressure distillation. Therefore, the conventional process is one of the most energy intensive processes. For this reason, a number of researchers have been developing other separation processes, which can replace the distillation. Among the alternatives, separation based on π-complexation appears the most promising.

The early attempts for the separation of olefin/paraffin mixtures based on π-complexation employed liquid solutions containing silver (Ag^+) or cuprous (Cu^+) ions. Recently, efforts to find available sorbents and to prepare new sorbents for the separations of ethylene/ethane and propylene/propane by pressure swing adsorption, have appeared in the literature. Especially, Yang et al. have prepared several kinds of new solid sorbents for selective light olefin over corresponding paraffin via π-complexation; Ag^+-exchanged resins (Yang et al., 1995), monolayered CuCl/γ-alumina, monolayered CuCl/pillared clays (Chen et al., 1995) and monolayered $AgNO_3/SiO_2$ (Padin et al., 2000). Cho et al. (2001) prepared π-complexation adsorbent by dispersing $AgNO_3$ on clay substrate.

Though the adsorbent gave high adsorption capacity and selectivity for ethylene compared to the commercial adsorbents like zeolite, it showed adsorption-desorption hysteresis so that the adsorption capacity of fresh adsorbent could not be fully utilized in cycle operation. To overcome the problem, new π-complexation adsorbent was prepared by dispersing $AgNO_3$ on aluminosilica substrate (Son et al., 2003). The adsorbent which is called $AgNO_3$/ALSG showed higher adsorption capacity for ethylene than $AgNO_3$/clay. Furthermore, reversibility of adsorption-desorption was superior to $AgNO_3$/clay. However, since $AgNO_3$/ALSG

*To whom correspondence should be addressed.

Table 1. Physical properties of substrates and prepared adsorbents.

Material	Average pore size (A)	BET surface area (m^2/g)	Pore volume (cm^3/g)
Clay	40.3	392	0.42
$AgNO_3$/clay	34.0	172	0.23
ALSG	28.9	719	0.52
$AgNO_3$/ALSG	32.9	268	0.22

adsorbed more ethane than $AgNO_3$/clay, the adsorption capacity ratios of ethylene to ethane of two sorbents were similar. In this study, performances of above two π-complexation adsorbents will be compared by simulation. Better sorbent for ethylene separation will be identified.

2. Adsorption Preparation

Adsorbents compared in this study are prepared by dispersing $AgNO_3$ on the clay and aluminosilica substrates.

Incipient wetness method was utilized in preparing the π-complexation adsorbent. The detail recipe of preparation was found elsewhere (Cho et al., 2001). Average pore diameter, BET surface area and pore volume of the substrates and the corresponding π-complexation adsorbents were given in Table 1. Average pore diameter of clay substrate is larger than that of aluminosilica substrate. After dispersing $AgNO_3$, the BET surface area and pore volume are reduced due to the blockage of the micropores.

3. Mathematical Model

The mathematical model adopted is a non-isothermal, non-equilibrium, bulk separation model. The assumption used to derive the model included the following: ideal gas behavior; no axial dispersion and no axial heat conduction; thermal equilibrium between gas phase and adsorbents. Mass transfer is represented by the linear driving force (LDF) approximation.

Based on the above assumptions, the mass balance for each component of the mixture and the total mass balance are written as follows:

Component mass balance

$$\frac{\partial y_i}{\partial t} + u\frac{\partial y_i}{\partial z} + \frac{(1-\varepsilon)}{\varepsilon}\rho_p \frac{R_g T}{P}\frac{\partial \bar{q}_i}{\partial t} - y_i \sum_j \frac{(1-\varepsilon)}{\varepsilon}\rho_p \frac{R_g T}{P}\frac{\partial \bar{q}_j}{\partial t} = 0 \qquad (1)$$

Total mass balance:

$$\frac{\partial C}{\partial t} + \frac{\partial (uC)}{\partial z} + \sum_i \frac{1-\varepsilon}{\varepsilon}\rho_p \frac{\partial \bar{q}_i}{\partial t} = 0 \qquad (2)$$

Energy balance for the gas phase includes the heat transfer to the column wall:

$$(\varepsilon c_{pg} C + (1-\varepsilon)c_{ps}\rho_p)\frac{\partial T}{\partial t} + \varepsilon c_{pg} u C \frac{\partial T}{\partial z} - \sum_i (-\Delta H_a)_i (1-\varepsilon)\rho_p \frac{\partial \bar{q}_i}{\partial t} + \frac{2h_w}{R_i}(T - T_w) = 0 \qquad (3)$$

In Eq. (3), the last term accounts for the heat transfer to the column wall. Energy balance around the column wall is given by

$$c_{pw}\rho_w a_w \frac{\partial T_w}{\partial t} = 2\pi h_w R_i (T - T_w) - 2\pi U_w R_o (T_w - T_F) \qquad (4)$$

Mass transfer is expressed by the LDF approximation.

$$\frac{\partial \bar{q}_i}{\partial t} = k_i (q_i^* - \bar{q}_i) \qquad (5)$$

The steady state momentum balance is given by Ergun's equation as follow:

$$-\frac{\partial P}{\partial z} = \frac{150\mu u}{d_p^2}\frac{(1-\varepsilon)^2}{\varepsilon^2} + 1.75\rho_g u^2 \frac{1-\varepsilon}{d_p \varepsilon} \qquad (6)$$

4. Results and Discussion

4.1. Pure Component Adsorption Isotherms

Pure component isotherms of ethane and ethylene on $AgNO_3$/clay and $AgNO_3$/ALSG at 25 ^{o}C are compared in Fig. 1. Adsorption isotherms of ethane and ethylene are fitted by the following models (Yang et al., 1995) and the results are shown in the figure as well.

$$q^*_{C_2H_6} = \frac{q_{si} b_i p_i}{1 + b_i p_i} \qquad (7)$$

$$q^*_{C_2H_4} = \frac{q_{si} b_i p_i}{1 + b_i p_i} + \frac{q_{sc}}{2s}\ln\left(\frac{1 + b_c p_i e^{s}}{1 + b_c p_i e^{-s}}\right) \qquad (8)$$

In Eq. (8), the second term of RHS represents the adsorption amount via π-complexation. Both adsorbents show high selectivity toward ethylene compared

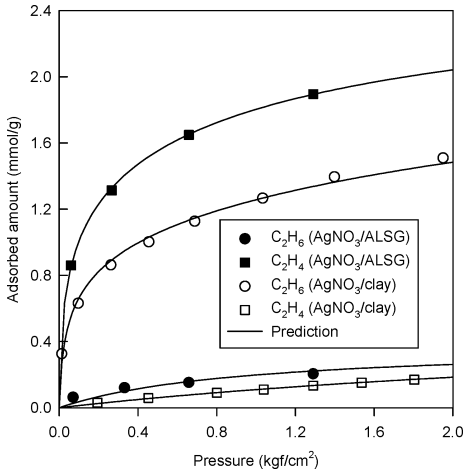

Figure 1. Adsorption isotherms of ethane and ethylene at 25°C

to the commercial adsorbents. As shown in the figure, $AgNO_3$/ALSG adsorbent has larger adsorption capacity for ethylene than $AgNO_3$/clay adsorbent. But, since $AgNO_3$/ALSG adsorbs more ethane than $AgNO_3$/clay, the adsorption capacity ratio, q_{C2H4}/q_{C2H6}, of two adsorbents at 1 atm are similar each other.

4.2. *Binary Adsorption Equilibrium*

Binary adsorption equilibrium of ethylene and ethane was measured at 25°C and 900 mmHg, and the results are shown in Fig. 2. Lines shown in the figure are the predicted with the following models.

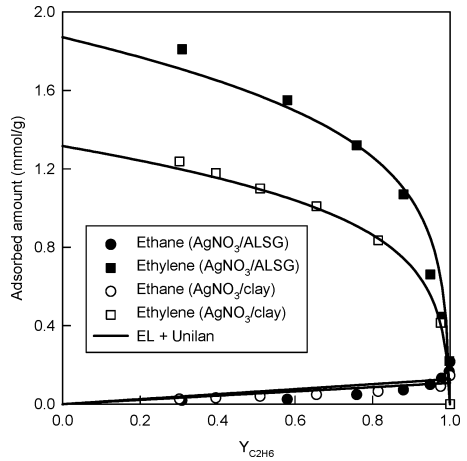

Figure 2. Binary adsorption equilibrium of ethane/ethylene at 25°C and 900 mmHg.

Equilibrium models shown in Eqs. (9) and (10) are the simple extension of pure component adsorption isotherm.

$$q^*_{C_2H_6} = \frac{\alpha \cdot q_{si} b_i p_i}{1 + \sum_j b_j p_j} \tag{9}$$

$$q^*_{C_2H_4} = \frac{\alpha \cdot q_{si} b_i p_i}{1 + \sum_j b_j p_j} + \frac{q_{sc}}{2s} \ln\left(\frac{1 + b_c p_i e^s}{1 + b_c p_i e^{-s}}\right) \tag{10}$$

In case of ethane, for which physical adsorption is dominant, the extended Langmuir model was used with a correction factor, α. Pure component adsorption isotherm of ethane shown in Fig. 2 consists of the physical adsorption of ethane on both the silver nitrate and bare surface of substrate. Ethane adsorbed on silver nitrate surface is easily displaced by ethylene even when small amount of ethylene exists in the gas phase. α was introduced to account for the physical adsorption on the $AgNO_3$ surface. Best fitting parameter of α was 0.5 for $AgNO_3$/ALSG and $AgNO_3$/clay. Selectivity for ethylene over ethane on the two adsorbents is shown in Fig. 3. It is clear from the figure that the $AgNO_3$/ALSG is more selective for ethylene than $AgNO_3$/clay especially in low ethane concentration. Since the source of ethylene/ethane mixture in industry contains high concentration of ethylene, $AgNO_3$/ALSG is better adsorbent in view of the selectivity and adsorption capacity.

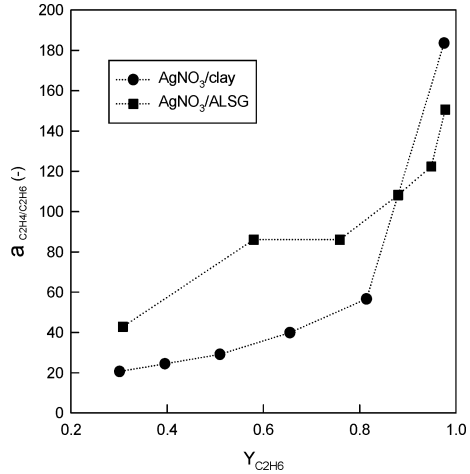

Figure 3. Selectivity of two adsorbent for ethylene at 25°C and 900 mmHg.

Table 2. Cycle sequence of 3-bed VSA process.

Time(s)	100	5	45	100	5	45	100	5	45
BED-1	AD			Rinse	EQ		EV	EQ	BF
BED-2	EV	EQ	BF	AD			Rinse	EQ	EV
BED-3	Rinse	EQ		EV		EQ	BF	AD	

AD: adsorption step, BF: back fill step, EQ: pressure equalization step, EV: evacuation step.

4.3. 3-Bed VSA Process

A 3-bed VSA cycle performance with $AgNO_3$/clay by simulation was compared with $AgNO_3$/ALSG. Simulation was performed under the conditions that the adsorption and desorption pressures, and feed flow rate were 1050 mmHg, 20 mmHg and 3000 mL/min, respectively. The cycle sequence of the 3-bed VSA process is shown in Table 2. The performance curves shown in Fig. 4 were obtained varying the rinse flow rate. Therefore, higher purity of ethylene shown in the figure corresponds to the higher rinse flow rate.

At relatively low purity of ethylene, about 99%, the recovery obtained with $AgNO_3$/clay is almost the same as that obtained with $AgNO_3$/ALSG. However, the superiority of $AgNO_3$/ALSG becomes clear as the purity of ethylene increases. At ethylene purity of 99.9%, the difference of recovery between $AgNO_3$/clay and $AgNO_3$/ALSG is about 4%. According to the simulation, ethylene purity of 99.9% can be produced with the recovery of 86% with $AgNO_3$/ALSG, and 82% with $AgNO_3$/clay.

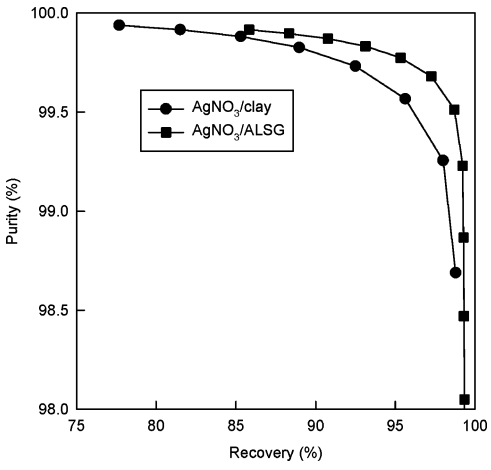

Figure 4. Performance of 3-bed VSA process (P_{AD}: 1050 mm Hg, P_{DE}: 20 mm Hg).

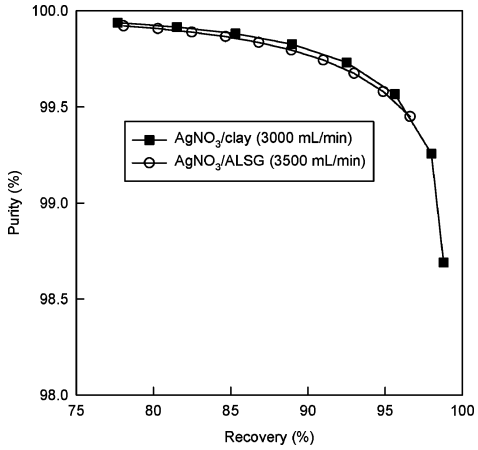

Figure 5. Comparison of performance of $AgNO_3$/clay and $AgNO_3$/ALSG (Feed flow rates in two simulations are different).

Since the working capacity of $AgNO_3$/ALSG is higher than that of $AgNO_3$/clay, higher rinse flow rate is required to produce the same purity of ethylene with $AgNO_3$/ALSG as that with $AgNO_3$/clay. To produce the ethylene purity of 99.9% with $AgNO_3$/ALSG, rinse flow rate of 2200 ml/min is required, but with $AgNO_3$/clay 1100 ml/min is sufficient.

To compare the performance of two adsorbents in terms of the productivity, simulation was performed for a 3-bed vacuum swing adsorption process using $AgNO_3$/ALSG adsorbent at different feed flow rate and compared the results to the $AgNO_3$/clay. The results are compared in Fig. 5. As shown in Fig. 5, the process using $AgNO_3$/ALSG gives similar performance even at higher feed flow rate. Since the cycle times of the two simulations are the same, the productivity of the process is solely determined by the feed flow rate and the recovery. Therefore, the productivity of the process with $AgNO_3$/ALSG is higher by 16% than that with $AgNO_3$/clay.

Acknowledgments

This research was supported by Korea Institute of Science & Technology Evaluation and Planning (KISTEP) under National Research Laboratory (NRL) program.

References

Chen, J.P. and R.T. Yang, "Molecular Orbital Study of Selective Adsorption of Simple Hydrocarbons on Ag^+ and Cu^+ Exchanged Resins and Halides," *Langmuir*, **11**, 3450–3456 (1995).

Cho, S.H., S.S. Han, J.N. Kim, N.V. Choudary, P. Kumar and S.G.T. Bhat, "Adsorbents, Methods for the Preparation and Method for the Separation of Unsaturated Hydrocarbons for Mixed Gases," US Patent, 6315816 B1 (2001).

Padin, J. and R.T. Yang, "New Aadsorbents for Olefin/Paraffin Separations by Adsorption via π-Complexation: Synthesis and Effects of substrates," *Chem. Eng. Sci*., **55**, 2607–2616 (2000).

Son, Y.R., S.S. Han, J.H. Park, J.N. Kim, S.H. Cho, and T.J. Lee, "Study on the Adsorption Characteristics of Light Hydrocarbons on Aluminosilica Based Sorbent," *HWAHAK KONGHAK*, **41**(6), 749–755 (2003).

Yang, R.T. and E.S. Kikkinides, "New Sorbents for Olefin/Paraffin Separations by Adsorption via π-Complexation," *AIChE J*., **41**(3), 509–517 (1995).